Project ID: **Fly-Radar**

Project Title: *"Low-frequency multi-mode (SAR and penetrating) radar onboard light-weight UAV for Earth and Planetary exploration"*

Call: **H2020-MSCA-RISE-2020**

WP1 – Mars Surface and subsurface analyses and terrestrial analogs

D1.5: DESCRIPTION AND SIMULATION OF GPR INVESTIGATION IN A MARTIAN ENVIRONMENT

Lead contributor	UCBL - (P. Allemand)
Other contributors	

Due date	31 January 2023
Delivery date	**07 February 2023**
Deliverable type	Report
Dissemination level	PU

Document History

Versio	Date	Description
Vs1.1	07 February	Final

This project has received funding from the European Union's Horizon 2020 research and innovation programme under MSCA-RISE2020 grant agreement No 101007973.

This deliverable presents models of the response of the FlyRadar instrument to different lithological and geometric configurations of the Martian subsurface. The GprMax software was used to model the response of a lava tube, ice lenses, a horizontal layer and an inclined layer. In addition, the effects of surface roughness were also evaluated. Model results show that each modelled object produces a backscattered signal that can be recorded by the instrument. The surface roughness does not alter the quality of the signal. The models produced are simplified cases since the transmitting and receiving antennas are not modelled. Similarly, the complexity of geological cases has been simplified to evaluate only the response of geological objects. This instrument will now have to be tested in terrestrial conditions.

2. Introduction

The objective of this deliverable is to demonstrate the capabilities of the FlyRadar instrument to study the geology of the first 10^{th} of meters of the Martian crust. Previous WP1 documents have shown the geological diversity of the Martian subsurface. This diversity is expressed through contrasting lithologies and varied geometries. The FlyRadar instrument is expected to produce data that will improve our knowledge of the planet in an area of major interests where life potentially occurred. Knowledge of Martian sub-surface is also essential since it will be the place of exploitation of minerals and water resources in the case of a human mission. Numerical modeling as the method was chosen to assess the efficiency of the FlyRadar instrument. Indeed, the physics of the radar signal is perfectly described by Maxwell's equations [Warren et al., 2016] which explain, among other things, the relationships between the electric field and the magnetic field induced by the propagation of an electromagnetic wave. Maxwell's equations present analytical solutions in simple cases and can also be solved by finite difference numerical methods in cases with complex geometries. We have therefore chosen to use a numerical solver of Maxwell's equations in complex geometry. In this document, we describe the solver, its usage and its limits, then we will detail our modeling strategy before presenting 5 families of results illustrating the diversity of Martian cases. This deliverable ends with a discussion of the potential of the FlyRadar tool.

3. Method: Numerical modelling

3.1 GprMax Description

GprMax [Warren et al., 2016] is an open source solver for modelling the propagation of electromagnetic waves in heterogeneous media. GprMax solves Maxwell's equations in a 3-dimensional physical space using the finite difference technique. The space is discretized by regular meshes making it possible to manage complex geometries. GprMax allows the modeling of basements with complex geometries taking into account the electromagnetic parameters. Similarly, it is possible to model the characteristics of sources as well as signal transmission and reception antennas. The program uses as input a geometric and electromagnetic description of the modelled area, a description of the wave source, as well as modeling parameters such as the dimensions of the meshes and the simulated duration.

The time step is determined to ensure the accuracy of the results and to avoid numerical discrepancies. The boundary conditions of the system are absorbing in order to avoid any reflection of the waves on these boundaries. The calculations are iterative. Each iteration corresponds to a time step. This time step must respect the conditions such that a wave will not cross more than the totality of a mesh during a time step.

GprMax has already been used in 3D conditions to simulate the response of a localized aquifer in fluvioglacial and lacustrine sediments (Koyan and Tronicke, 2020). It is also used by Eide et al. (2021) and Eide et al. (2022) to model the Radar response of the possible underground features of the Jezero crater located on Mars and selected to be investigated by the Perseverance rover.

This project has received funding from the European Union's Horizon 2020 research and innovation programme under MSCA-RISE2020 grant agreement No 101007973.

GprMax uses a parameter file as input. These parameters define the geometry of the 3-dimensional model as well as the mesh size, the position of the transmitting antenna and the receiving antenna, the dielectric constants of the constituent media, the characteristics of the wave emitted, the modelled duration. It is possible to obtain results from a 1D survey (A-scan) or from a 2D profile (B-scan) (Phaebua et al., 2022). The dielectric parameters are chosen according the environment (ElShafie and Heggy, 2013). The source is a broadband Ricker wavelet with 80 MHz center frequency.

The gprMax results were compared with analytical results (fig. 1). The agreement between the two families of solutions is excellent. This demonstrates the quality of gprMax and its interest in modeling the FlyRadar tool.

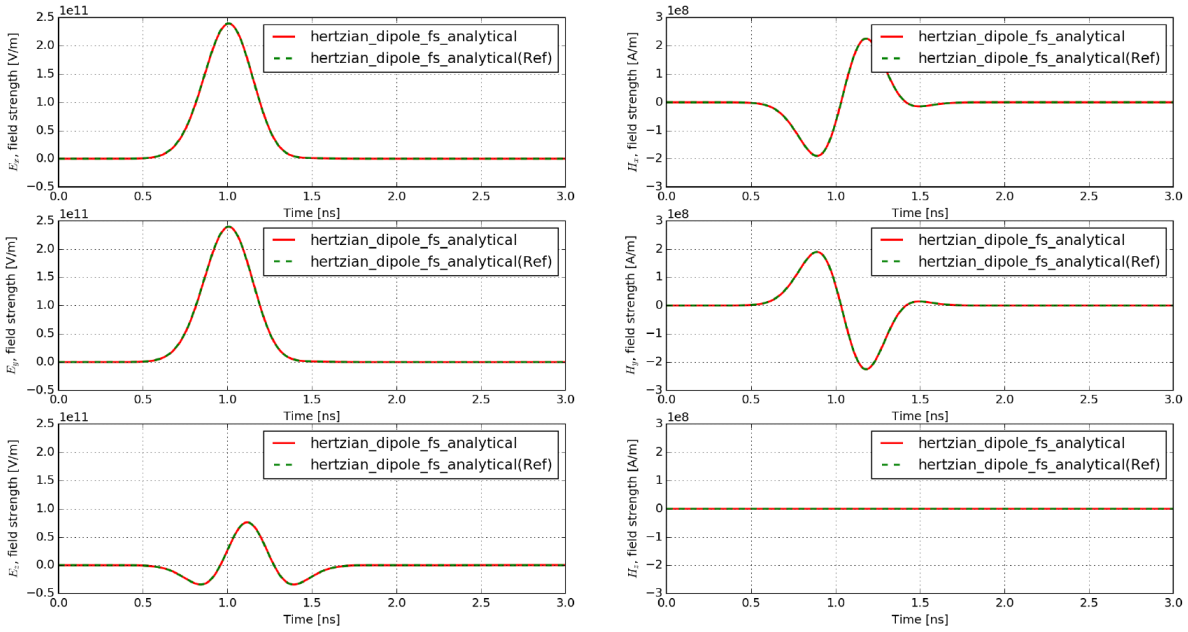

Figure 1: Comparison of the numerical results produced by gprMax compared to an analytical solution in the case of the propagation of a Gaussian wave train with a wavelength centered on 1 GHz.

3.2 Modelling strategy

Five geometries were selected to represent the diversity of geological cases possibly encountered on Mars. The effect of geometric parameters (depth, angle, thickness, cavity radius, etc.) were tested. Likewise, the effect of the dielectric properties of the materials was evaluated in each case (Brouet, et al., 2019). Finally, the role of surface roughness has been modeled in the simple case of a horizontal layer. For each case, an A-scan (vertical sounding) was modeled directly below the antennas. A few B-Scans (cross section) were made in the clearly two-dimensional contexts.

The antennas are not accurately modeled in this work. These were considered as a simple transmitter spaced two meters from the receiver. The gain of the two antennas is not taken into account. However, to simulate this gain, it was assumed that the receiver could record signals attenuated less than -150 dB relative to the source.

4. Results

In all of the following simulations, the FlyRadar instrument is assumed to be flying 3 m above the surface, in the middle of the model. The transmitting antenna is located 2 m from the receiving antenna. The wave train emitted has a Rickert shape (Mexican hat) with a duration of 4 nanoseconds and centered on 80 MHz. The modeled domain is 15 m long (X horizontal axis) by 35 m high (Y vertical axis) and 0.02 m thick (Z horizontal axis). The

This project has received funding from the European Union's Horizon 2020 research and innovation programme under MSCA-RISE2020 grant agreement No 101007973.

upper part of the model is occupied by a layer of atmosphere 8 m thick. A similar configuration has already been used on Earth with good results (Thakur and Bruzzone, 2019).

4.1 Detection of a lava tube on Mars

The response of a lava tube located in a basalt flow is modelled. The parameters tested are the diameter and the depth of the tube. The interior of the tube is made of a material having the properties of vacuum. The surrounding rock has the dielectric properties of a basalt (relative permittivity of 8).

Figure 2 illustrates the results. This figure shows the different components of the electric (V/m) and magnetic (A/m) fields received by the instrument in the case of a lava tunnel 5 meters in diameter which center is located at a depth of 10m. The horizontal axes mark the time and the vertical axes the intensity of the reflected signals. The first signals that arrive are the most intense. They are produced by reflections on the ground. The median frequency (f) being 80 MHz, the wavelength (λ=c/f) is about 3.75 m (c is the velocity of electromagnetic waves). Such a wavelength does not allow precise positioning of objects but has the advantage of being very penetrating. The following wave train marks the reflections on the roof and inside the cavity. Knowing the return time of the wave and with an estimate of the relative permittivity of the rocky medium, it is then possible to estimate the depth of the cavity. It is noted that the signal from the cavity is very attenuated along the y component of the electric field. This depends on the orientation of the antennas. There is also a very strong attenuation of the magnetic field.

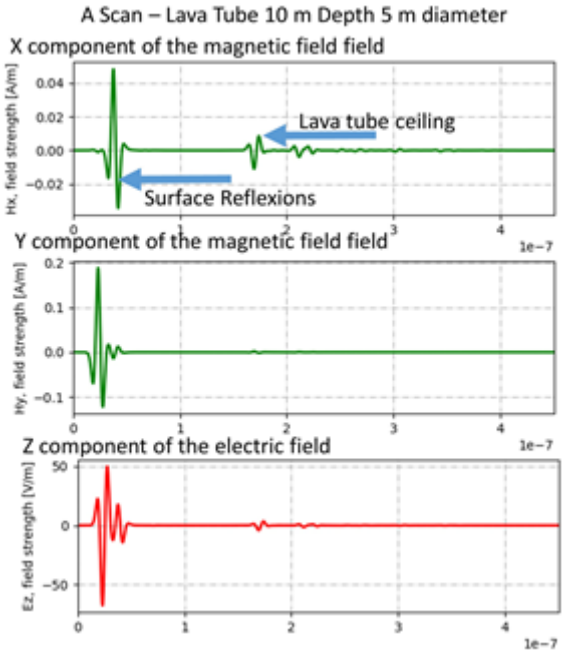

Figure 2: Example of a A-scan above a lava tube with a diameter of 5 m with a center located at 10 m depth.

Figure 3 shows the A-scans for a series of geometric parameters of the lava tube. The diameter is 1, 3 or 5 m and the depth is 2, 5, 10 or 20 m. The electric and magnetic field strength is shown for each example. A signal appears in each case, in particular for the y component of the electric field. When the tube is too shallow, its response merges with the surface signal.

This project has received funding from the European Union's Horizon 2020 research and innovation programme under MSCA-RISE2020 grant agreement No 101007973.

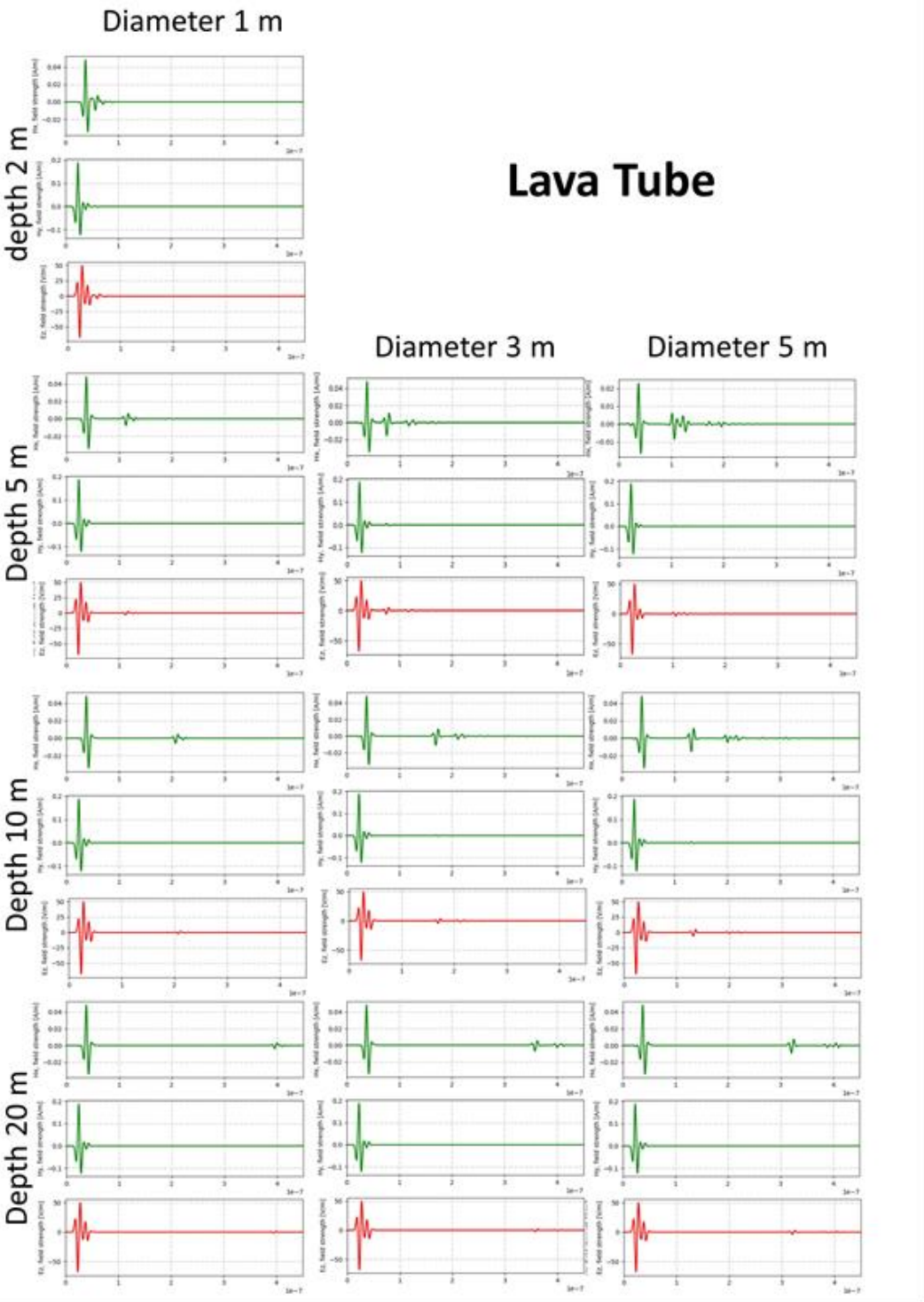

Figure 3: A-scans of a lava tube in a volcanic layer.The lava tubes are elongated perpendicularly to the figures. Their diameter varies from 1 to 5 m and the depth of the center of the tube varies from 1 to 20 m. The x and y components of the electric field and the z component of the mangetic field are presented. The response of the lava tubes is visible on each x component of the electric field. The response of the 1 m diameter lava tube located at 2 m depth merges with surface reflexions.

This project has received funding from the European Union's Horizon 2020 research and innovation programme under MSCA-RISE2020 grant agreement No 101007973.

4.2 Lens of ice in a lava flow

This example illustrates the potential of the FlyRadar instrument for detecting circular ice lenses embedded in a basaltic layer. The depths of the center of the lenses are 2, 5, 10 and 20 m respectively. The diameter of the lenses is 1, 3 and 5 meters respectively. The effect of the lenses is visible in each case on the y component of the electric field.

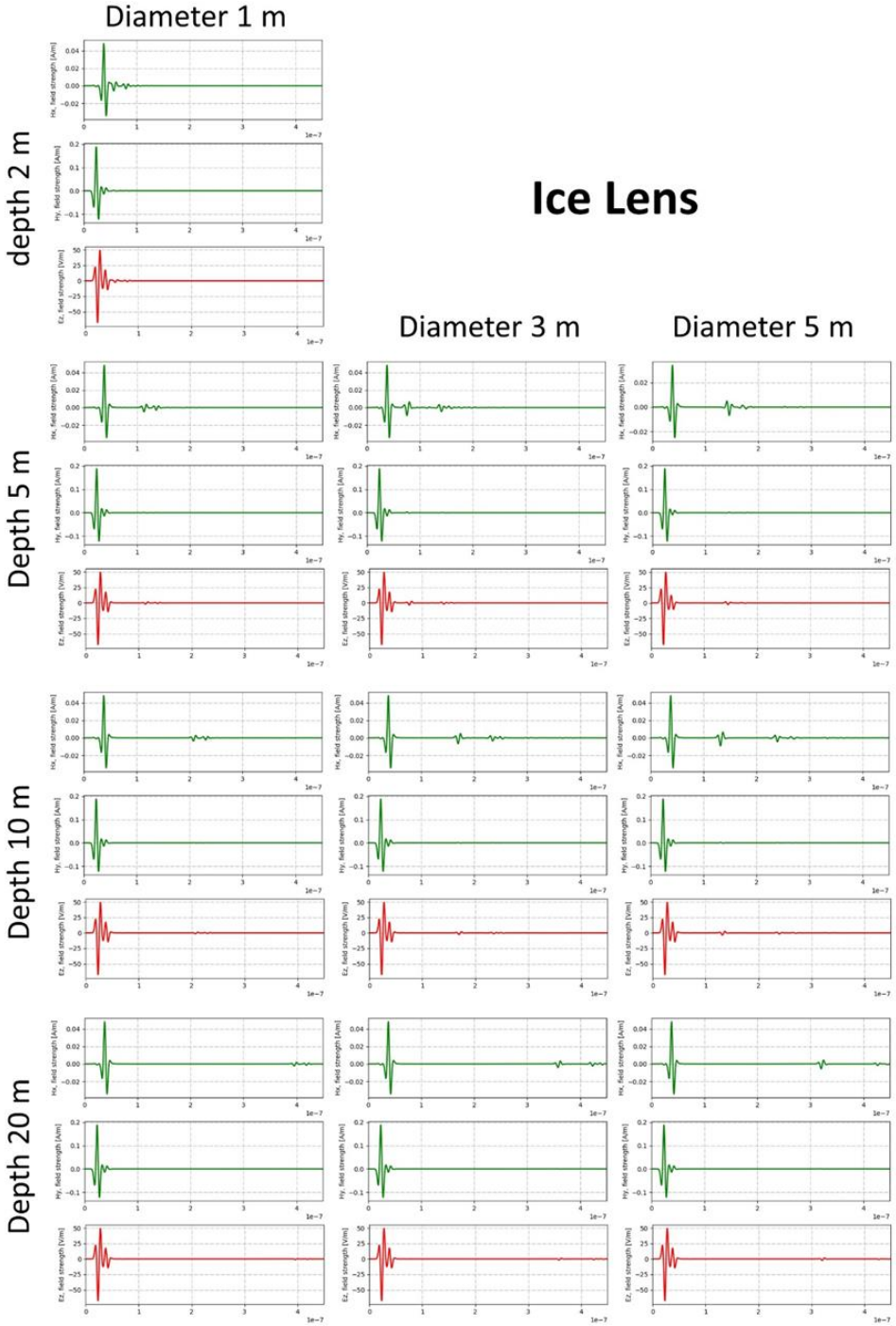

Figure 4: Response of the FlyRadar instrument to the presence of an ice lens in a basalt flow. The parameters are the diameter of the lens and its depth. The lens affects the signal picked up by the instrument. For a lens located at low depth, the signal merges with the signals reflected at the surface.

This project has received funding from the European Union's Horizon 2020 research and innovation programme under MSCA-RISE2020 grant agreement No 101007973.

A section of the response of the FlyRadar instrument was calculated on the example of an ice lens 3 m in diameter whose center is located 10 m below the surface (fig. 5). A characteristic response with a hyperbola is clearly visible.

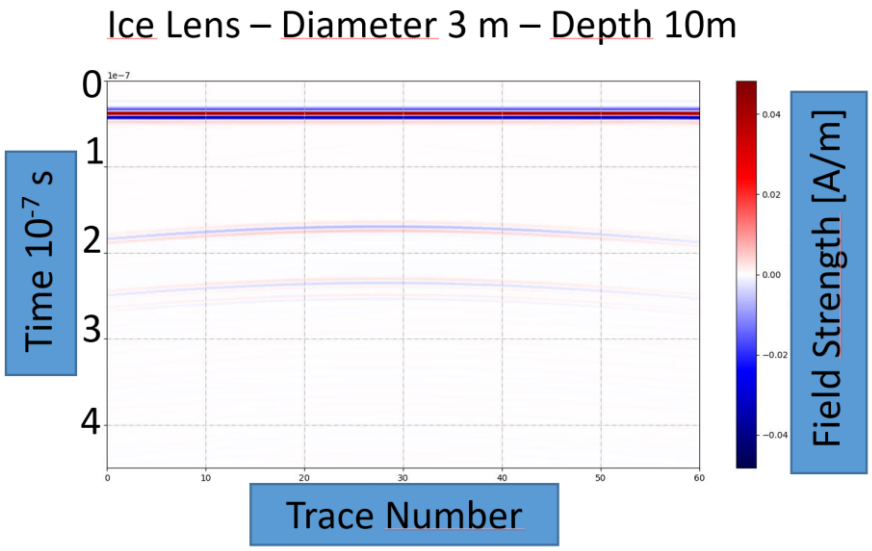

Figure 5: Section of the response of an ice lens 3 m in diameter located at 10 m depth. A characteristic hyperbola and its replicas are visible in the image.

4.3 Case of a horizontal layer

The case of a horizontal permittivity interface has been modelled. The parameters are the interface depth (2, 5, 10 and 20 m) and the permittivity contrast between the surface layer and the deeper basement (relative permittivity contrast of 3/8 and 5/8). The results of vertical soundings are given in figure 6.

This project has received funding from the European Union's Horizon 2020 research and innovation programme under MSCA-RISE2020 grant agreement No 101007973.

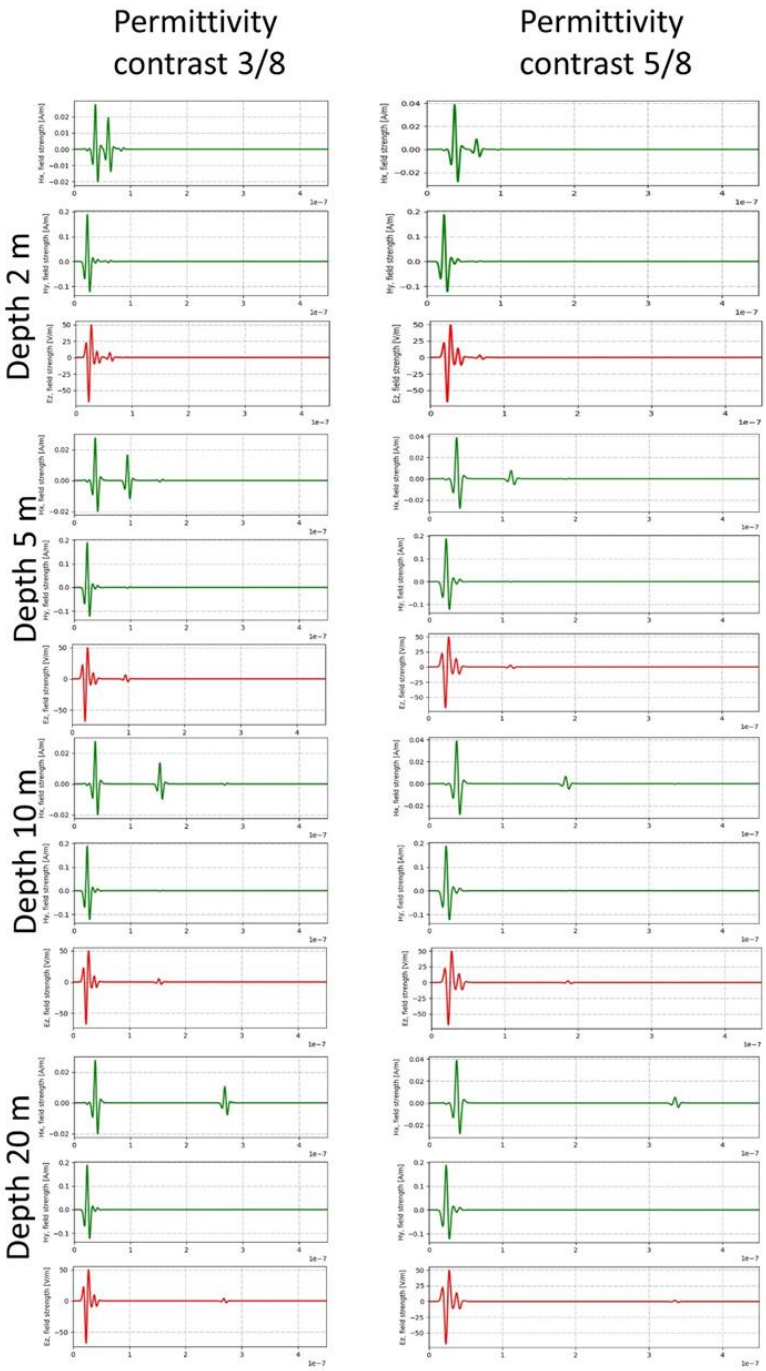

Figure 6: Response of the FlyRadar instrument to the presence of a horizontal permittivity contrast in the underground. The parameters are the depth of the interface and the permittivity contrast between the surface layer and the basement. The interface is visible up to 20 m depth. The signal is less intense when the permittivity contrast is lower.

4.4 Case of an inclined layer

The presence of a tilted permittivity interface has been modelled. The parameters are the dip of the interface (18, 25 and 31°). The permittivity contrast between the surface layer and the deeper bedrock is 3/8. This contrast is the

This project has received funding from the European Union's Horizon 2020 research and innovation programme under MSCA-RISE2020 grant agreement No 101007973.

most favorable to detection (see detection of horizontal interfaces). The results of vertical soundings are given in figure 7. The 18° dipping interface produces a weakly visible signal. Higher dipping interfaces produce no signal and are therefore not detectable.

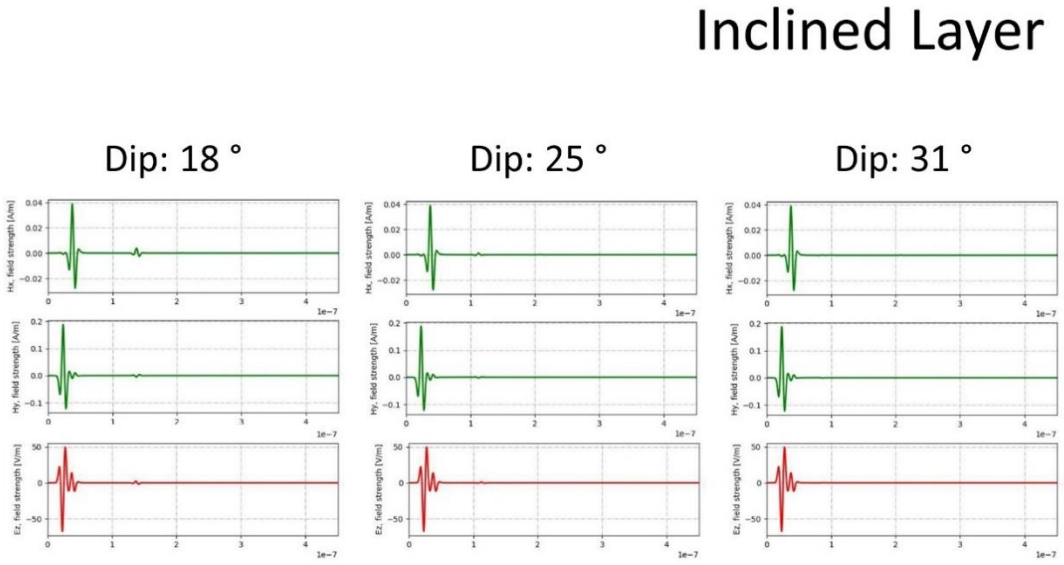

Figure 7: Response of the FlyRadar instrument to the presence of a tilted permittivity contrast in the underground. An 18° sloped interface is visible. Higher slope interfaces produce no signal.

A section was made for the 18° dip case. The permittivity interface is visible (Figure 8). Knowing the relative permittivity, it is possible to estimate the dip of the layer in such case.

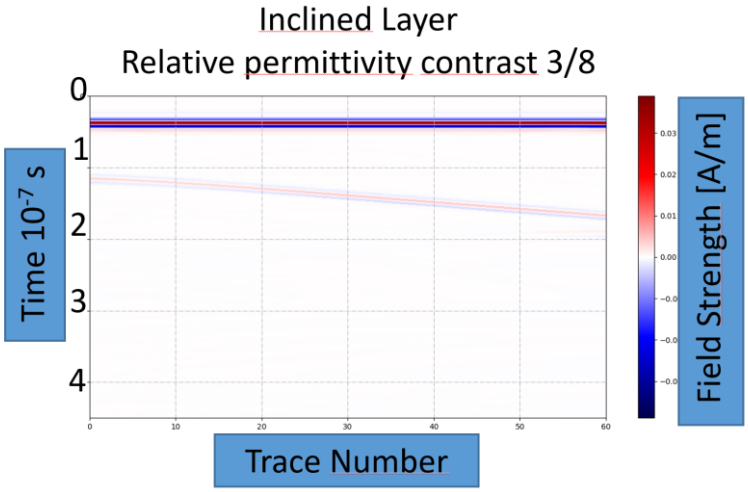

Figure 8: Simulated section of the response of an 18° tilted permittivity interface. The permittivity contrast is 3/8. The interface between the two media is visible all along the section.

4.5 Effect of surface roughness

In previous models, the interface between rocks and the atmosphere is considered smooth. However, in nature, the surface is generally rough that is covered by different elements of various sizes and height. This roughness will backscatter incoming signal which will decrease in intensity. GprMax is able to integrate surface roughness in the calculations. The surface is assimilated to a fractal surface whose size it is possible to parameterize for the

This project has received funding from the European Union's Horizon 2020 research and innovation programme under MSCA-RISE2020 grant agreement No 101007973.

largest and smallest objects. Simulations were conducted to assess the role of surface roughness on the response of the FlyRadar instrument (fig. 9). The simulation conditions are equivalent to those described in the case of the detection of a lava tunnel. A circular tunnel 5 m in diameter is located 10 m deep. The minimum roughness takes the values of 0.01 m, 0.1 m and 0.5 m. The maximum roughness takes the values of 0.1 m, 0.5 m, 1 m. No clear effect of the roughness is registred in the signal.

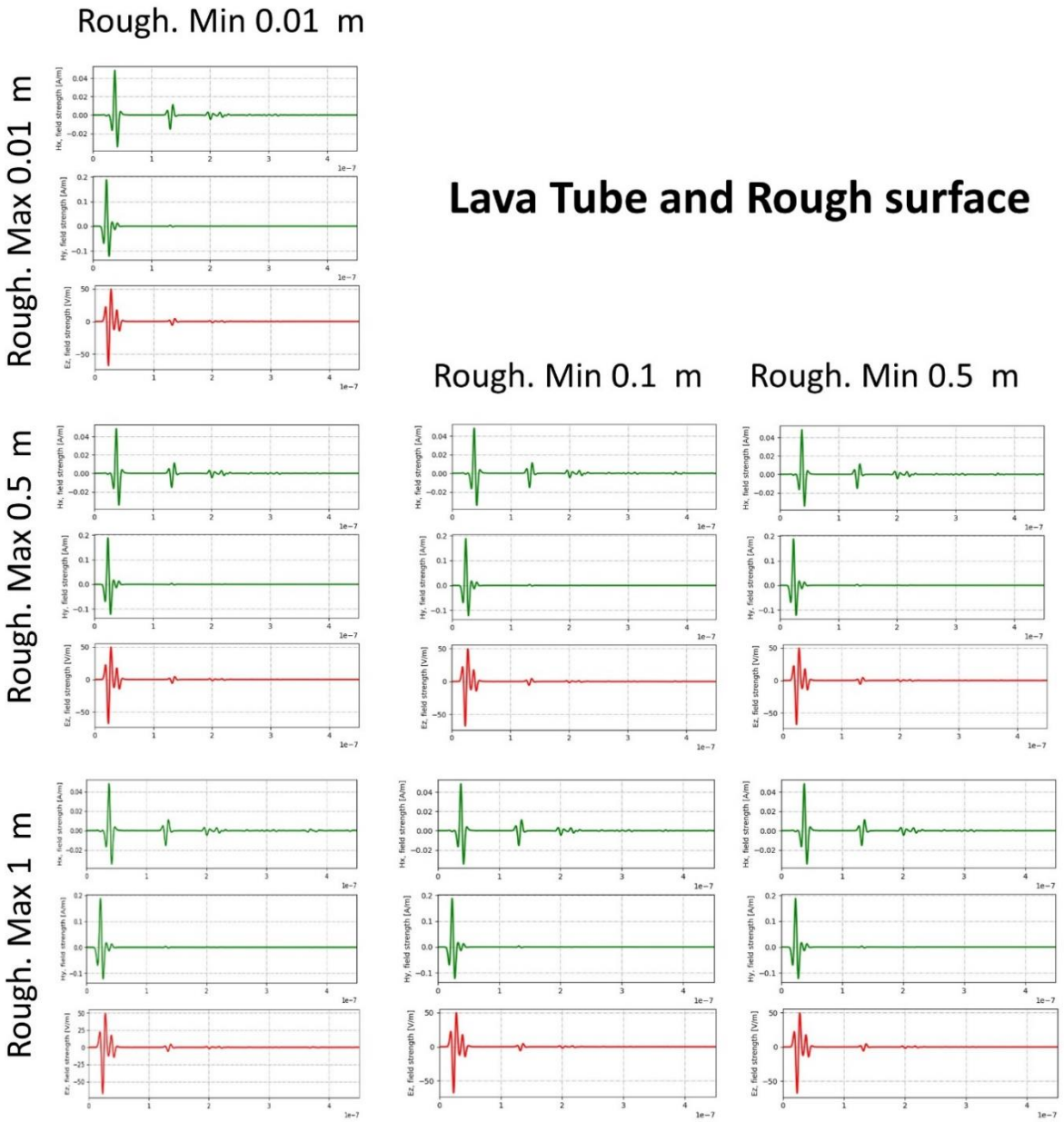

Figure 9: Effect of surface roughness on the signal of the FlyRadar instrument. No clear effect is detected. The frequency of the radar is low enough that the electromagnetic waves are not affected by surface roughness in the range of 0.01 to 1 m.

This project has received funding from the European Union's Horizon 2020 research and innovation programme under MSCA-RISE2020 grant agreement No 101007973.

5. Discussion

It is shown in this document that in the majority of the cases studied, the FlyRadar tool records a reflected signal if it is placed at 3 m above the ground. This result is confirmed by the results of the cross-section models which demonstrate that the objects and heterogeneities of the subsoil are recorded and visible. In addition, the frequency used (80 MHz) makes the signal insensitive to surface roughness. A signal acquired on a rough area is similar, in the first order, to a signal acquired on a smooth area. Sloped layers are detected if the slope is less than 18°. For higher slopes, the signal is reflected in such a way that the receiving antenna no longer picks it up. This is a classic bias of the radar sounding method. Flyradar tool seems suitable for searching for cavities, ice lenses and plane permittivity interfaces. It therefore has excellent potential for use in Martian exploration.

However, some limitations to the modeling presented here should be noted. First of all, the transmitting and receiving antennas have not been integrated. The role of an antenna is to amplify the signal. Our models without antenna therefore underestimate the potential of the instrument. The cutoff of a received signal at -150dB that we use in our models could be too elevated to be representative of the instrument.

The second limitation of our modelling concerns the way by which we model the underground. In our models, the underground is a perfect media devoid of heterogeneities of dielectric constants produced by fractures or lithological local variations. Moreover, we do not take into account the effect of oxides and possible microscopic bound water content that attenuate the radar signal.

The third limitation of our models, is that the UAV is not taken into account. Only tests in real conditions will permit to evaluate the possible interactions between the electromagnetic fields of the instrument and those of the UAV.

5. Conclusion

Despite some limitations, numerical simulations of the responses of the FlyRadar instrument in various geological contexts show that the instrument is suitable for the study and exploration of the Martian underground. The results of the models show that the FlyRadar instrument in its setup will be able to detect a signal from a lava tube, an ice lense and a horizontal permittivity interface even if the surface is rough at meter scale. The instrument does not detect inclined layers if their slope is of 25° or more. This non-detection is inherent to the method and not specific to the FlyRadar instrument.

6. Repository for primary data[1]

Model results are available on request.

7. References

Brouet, Y., Becerra, P., Sabouroux, P., Pommerol, A., & Thomas, N. (2019). A laboratory-based dielectric model for the radar sounding of the Martian subsurface. Icarus, 321, 960–973. https://doi.org/10.1016/j.icarus.2018.12.029

Eide, S., Hamran, S-E, Dypvik, H., & Amundsen, H.E.F. (2021). Ground-penetrating radar modeling across the Jezero crater floor, IEEE J. Sel. Topics Appl. Earth Observ. Remote Sens., vol. 14, pp. 2484–2493, https://doi.org/10.1109/JSTARS.2021.3055944.

[1] Suggested headings

This project has received funding from the European Union's Horizon 2020 research and innovation programme under MSCA-RISE2020 grant agreement No 101007973.

Eide, S., Casademont, T., Aardal, ØL & Hamran, SE. (2022). Modeling FMCW Radar for Subsurface Analysis. EEE J. Sel. Topics Appl. Earth Observ. Remote Sens., vol. 15, pp. 2998–3007, 2022, https://doi/10.1109/JSTARS.2022.3165135.

ElShafie, A., Heggy, E. (2013). Dielectric and hardness measurements of planetary analog rocks in support of in-situ subsurface sampling, Planetary and Space Science 86, 150–154, https//doi.org/10.1016/j.pss.2013.02.003.

Koyan, P., & Tronicke, J. (2020). 3D modeling of ground-penetrating radar data across a realistic sedimentary model, Comput. Geosci., vol. 137, https://doi.org/10.1016/j.cageo.2020.104422.

Phaebua, K., Lertwiriyaprapa, T., Burintramart, S., & Boonpooga, A. (2022) The B-Scan Image Simulation Method of a Ground-Penetrating Radar Mounted on a Drone Using a High-Frequency Technique. IEE Acess, vol. 10, https//doi.org/10.1109/ACCESS.2022.3188455.

Thakur, S., & Bruzzone, L. (2019). An Approach to the Simulation of Radar SounderRadargrams Based on Geological Analogs. IEEE Trans. Geosci. Remote Sens., vol. 57, no. 8, pp. 5266-5284, https://doi.org/10.1109/TGRS.2019.2898027.

Warren, C., Giannopoulos, A., & Giannakis I. (2016). gprMax: Open source software to simulate electromagnetic wave propagation for Ground Penetrating Radar, Computer Physics Communications, http://dx.doi.org/10.1016/j.cpc.2016.08.020.

This project has received funding from the European Union's Horizon 2020 research and innovation programme under MSCA-RISE2020 grant agreement No 101007973.